THE ASTROPHYSICAL JOURNAL, 482:519–534, 1997 June 10


# NEUTRAL-LINE MAGNETIC SHEAR AND ENHANCED CORONAL HEATING IN SOLAR ACTIVE REGIONS



D. A. FALCONER[1]
National Research Council/Marshall Space Flight Center
R. L. MOORE,[1] J. G. PORTER,[1] AND G. A. GARY[1]
NASA/Marshall Space Flight Center
AND
T. SHIMIZU
Institute of Astronomy, University of Tokyo, Mitaka, Tokyo 181, Japan
*Received 1996 July 15; accepted 1997 January 9*

## ABSTRACT

By examining the magnetic structure at sites in the bright coronal interiors of active regions that are not flaring but exhibit persistent strong coronal heating, we establish some new characteristics of the magnetic origins of this heating. We have examined the magnetic structure of these sites in five active regions, each of which was well observed by both the *Yohkoh* SXT and the Marshall Space Flight Center Vector Magnetograph and showed strong shear in its magnetic field along part of at least one neutral line (polarity inversion). Thus, we can assess whether this form of nonpotential field structure in active regions is a characteristic of the enhanced coronal heating and vice versa. From 27 orbits' worth of *Yohkoh* SXT images of the five active regions, we have obtained a sample of 94 persistently bright coronal features (bright in all images from a given orbit), 40 long ($\gtrsim$20,000 km) neutral-line segments having strong magnetic shear throughout (shear angle greater than 45°), and 39 long neutral-line segments having weak magnetic shear throughout (shear angle less than 45°). From this sample, we find that (1) all of our persistently bright coronal features are rooted in magnetic fields that are stronger than 150 G, (2) nearly all (95%) of these enhanced coronal features are rooted near neutral lines (closer than 10,000 km), (3) a great majority (80%) of the bright features are rooted near strong-shear portions of neutral lines, (4) a great majority (85%) of long strong-shear segments of neutral lines have persistently bright coronal features rooted near them, (5) a large minority (40%) of long weak-shear segments of neutral lines have persistently bright coronal features rooted near them, and (6) the brightness of a persistently bright coronal feature often changes greatly over a few hours. From these results, we conclude that most persistent enhanced heating of coronal loops in active regions (1) requires the presence of a polarity inversion in the magnetic field near at least one of the loop footpoints, (2) is greatly aided by the presence of strong shear in the core magnetic field along that neutral line, and (3) is controlled by some variable process that acts in this magnetic environment. We infer that this variable process is low-lying reconnection accompanying flux cancellation.

*Subject headings:* Sun: activity — Sun: corona — Sun: magnetic fields — sunspots — Sun: X-rays, gamma rays

## 1. INTRODUCTION

The top two panels of Figure 1 show a typical whole-Sun soft X-ray image taken by the Yohkoh Soft X-ray Telescope (SXT). This image demonstrates that in soft X-rays the entire outer solar atmosphere, the corona, greatly outshines the underlying photosphere, showing that the X-ray coronal plasma is maintained at temperatures of order $10^6$ K, hundreds of times hotter than the photosphere. The heating process that generates and sustains the observed hot corona remains unknown and is a long-standing problem of broad astrophysical importance.

*Skylab* X-ray, XUV, and EUV coronal images, in combination with magnetograms, have firmly established that coronal heating is a magnetic phenomenon (e.g., Vaiana & Rosner 1978). In the same way as Figure 1, the *Skylab* observations showed that the brightest nonflare features of the X-ray corona mark the strongest magnetic fields found on the Sun, which are found in active regions having sunspots. The coincidence of bright coronal X-ray features with magnetic field concentrations and the positive correlation of X-ray brightness with strength of the magnetic field suggest that coronal heating is a consequence of the magnetic field and hence that the heating is some form of electric current dissipation (e.g., Kuperus, Ionson, & Spicer 1981; Antiochos 1990). There are two broad possibilities for the character of the dissipating currents: they are either DC or AC (Narain & Ulmschneider 1996). For example, the currents that are dissipated in reconnection models of microflares and nanoflares (e.g., Parker 1988) are DC; the currents in MHD waves, such as Alfvén waves, fall in the AC category. Of course, there is a wide range of hybrid possibilities in which the heating is partly DC and partly AC. For example, a microflare may produce local coronal heating by DC dissipation and at the same time generate

[1] Space Science Laboratory, Code ES82, NASA/MSFC, Huntsville, AL 35812; falcoda@ips1.msfc.nasa.gov.

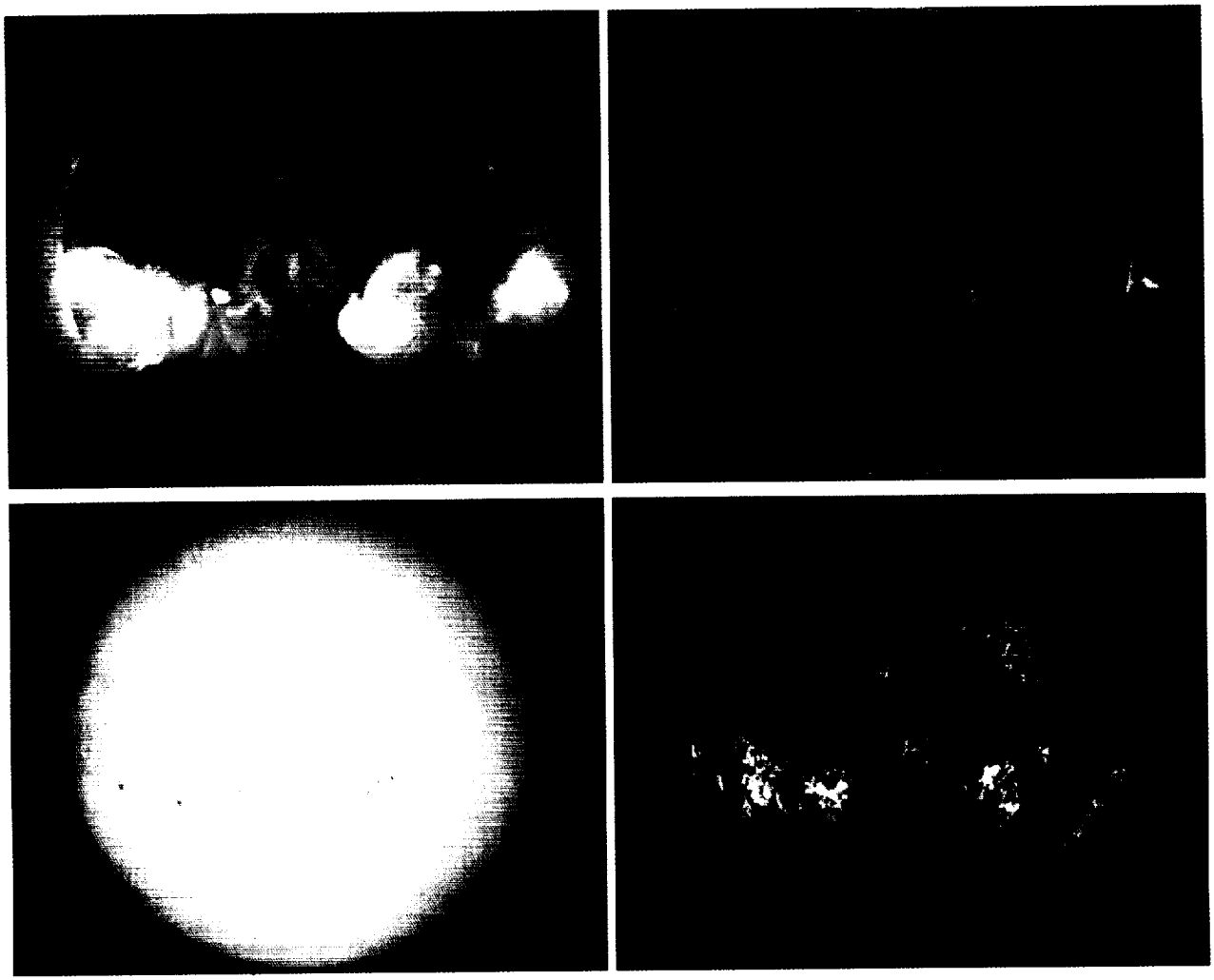

FIG. 1.—Whole-Sun images illustrating that coronal heating is a magnetic phenomenon: the strongest heating (brightest corona) is seen to be in the strong magnetic fields in sunspot regions. *Top left*: SXT coronal image displayed with logarithmic scaling of the brightness. This image shows that in quiet regions (everywhere outside of the strong-field active regions) the corona glows detectably in X-rays but is orders of magnitude dimmer than the bright interiors of active regions. This image is a composite of one exposure of 78 ms and one of 2668 ms taken through the thin aluminum filter at 16:53 and 16:57 UT, 1991 December 26. *Top right*: The same SXT coronal image displayed with square-root scaling to show the coronal structure in the bright active regions. From comparison with the magnetogram (*bottom right*), it is evident that the brightest coronal features in an active region cover only a fraction of the whole strong-field domain of the region. *Bottom left*: SXT photospheric image showing sunspots near the time (same orbit) of the coronal image in the top panels. *Bottom right*: Kitt Peak National Solar Observatory magnetogram taken on the same day, showing both the active-region concentrations of strong magnetic field and scattered, weaker fields in quiet regions. All four images have the same orientation: north is up, west is right.

MHD waves that propagate away to produce remote coronal heating in extended magnetic loops stemming from the site of the microflare. In the present study, we find that this particular DC/AC hybrid scenario is a viable possibility for much of the enhanced coronal heating in active regions. Our intent in the above remarks is not to review coronal heating mechanisms, but to remind the reader that, from elementary observations together with simple physical reasoning, it is quite plausible that coronal heating is closely connected with the nonpotentiality (and the corresponding electric currents) of the magnetic field in which the heating occurs. This thought, in turn, suggests that vector magnetograms, by virtue of showing the nonpotentiality of the magnetic field, might give useful clues for coronal heating.

Throughout this paper, we assume that coronal X-ray brightness increases with the coronal heating rate. This finding is appropriate to coronal magnetic loops, in which much of the coronal heating is balanced by coronal radiative cooling, as in the static models of Rosner, Tucker, & Vaiana (1978). That the active-region coronal loops observed by the *Yohkoh* SXT follow this rule has recently been confirmed by Kano & Tsuneta (1996).

The *Yohkoh* SXT more clearly shows the structure of the bright corona in active regions than the *Skylab* X-ray telescopes did, largely because there is less X-ray scattering by the optics in the *Yohkoh* SXT. We can see from even a cursory comparison of SXT coronal images with conventional magnetograms (maps of the line-of-sight component of the photospheric roots of the magnetic field), as in Figure 1, that the brightest coronal features in an active region occupy only some parts of the strong-field domain of the active region. While it is true that the brightest coronal features are seated in strong fields, there are other places in the active region where the field is as strong or stronger, but the corona is much dimmer, showing that the heating is much weaker. Thus, it is clear that the strength of the

enhanced heating in active regions depends on more than just the strength of the magnetic field. It would be surprising if the heating depended only on the strength of the field and not on any additional aspects of the magnetic environment. The intent of the present work is to find clues to these additional factors by examining the arrangement of the magnetic field at sites of strong coronal heating.

The present paper is a direct descendant of two exploratory papers, Moore et al. (1994) and Porter et al. (1994), which demonstrated that comparison of *Yohkoh* SXT images with Marshall Space Flight Center (MSFC) vector magnetograms could yield new clues to coronal heating. These initial papers were limited to two active regions and to only one orbit of SXT observations of each active region. The two active regions were selected for study because their vector magnetograms showed extensive strong shear in their core magnetic fields, that is, in the fields along the polarity dividing lines, the so-called neutral lines. The shear in the magnetic field is measured by the acute angle between the observed transverse field vector and the potential transverse field vector computed from the observed line-of-sight magnetic field of the entire active region; if the observed field is a potential field, this angle is zero; if the observed field is strongly sheared, this angle approaches 90° (Hagyard et al. 1984; Ambastha, Hagyard, & West 1993). Channels of neutral-line magnetic shear are a common form of nonpotentiality in active regions. When present, they are typically the most nonpotential fields in the active region. These strongly sheared core fields are often the seats of flares, which suggests that the free magnetic energy of the sheared field fuels these flares. This energy or its source might also be continually tapped for strong coronal heating so that, in the absence of any full-fledged flare, sheared core fields would be sites of persistent enhanced coronal features in the interiors of active regions. The purpose of the initial work that led to the first two papers was to test this expectation.

In the two active regions presented by Moore et al. (1994), the strongly sheared core fields stood out as bright features in the SXT coronal images. This result showed that there was enhanced coronal heating in these nonpotential magnetic fields, as had been anticipated. These coronal features were persistently bright over the 50 minute orbital span of the SXT observations that were analyzed in that study. While these features were, on the whole, persistently bright, substructures throughout them continually fluctuated in brightness on timescales of minutes, in the manner of microflaring. These fluctuations suggested that the hot coronal plasma in the sheared core fields was maintained by this continual microflaring activity, and that these microflares are similar to the full-fledged flares in sheared core fields in the way that they are triggered and burn in the sheared magnetic field.

Porter et al. (1994) focused on an unanticipated finding, namely that in addition to having enhanced coronal brightness in the sheared core fields, one of the active regions also had a cluster of extended bright loops that were rooted well away from the main neutral line of the overall bipolar active region and arched high over this neutral line. The brightness of these enhanced extended coronal loops was noticeably steadier than that in the sheared core fields. These bright extended loops stemmed from the vicinity of an island of included polarity in the magnetic flux. The magnetic field was strongly sheared at some places along the neutral line around this island, and these localized sheared core fields were sites of microflaring and enhanced coronal brightness. These observations suggested that the extended bright loops received enhanced coronal heating because they had one end near the magnetic island and that they were heated by MHD waves that were continually emitted up into them from the microflaring activity around the island.

Because only two active regions were examined in the two initial papers, we could not be sure that the observed connections of enhanced coronal heating to neutral-line magnetic shear and to microflaring were typical rather than exceptional. The intent of the present study is to answer this question with respect to neutral-line magnetic shear. Specifically, in the present study we seek to answer the following two questions:

1. Is neutral-line magnetic shear a reliable marker of enhanced coronal heating?
2. Is enhanced coronal heating a reliable marker of neutral-line magnetic shear?

To address these questions, we have enlarged our data set by including more active regions, more days per active region, and more orbits' worth of SXT images per day. As before, each active region was selected because it had at least some strong neutral-line shear. The set of active regions also includes a comparably large sampling of core magnetic fields having little shear, so that we can investigate the relationship between strength of neutral-line magnetic shear and intensity of enhanced coronal heating. In the present study we concentrate on the magnetic structure in and near persistently bright coronal features. We do not investigate in any detail the microflaring or lack of microflaring within the bright features; brightness variations on times of less than an orbit will be the focus of another study. From the present study, we find that the answer to both of our two questions above is "yes." Our results also show that while neutral-line magnetic shear may well have an active role in producing enhanced coronal heating, it does not act alone, but in concert with some hidden-variable agent that sets the heating rate and that can act only in the presence of a magnetic neutral line.

## 2. DATA ANALYSIS

### 2.1. *Data Set*

The MSFC vector magnetograph (Hagyard et al. 1982; West 1989; Hagyard, Cumings, & West 1985) records Stokes polarization images in the wings of the Fe I 5250.2 Å line. These images can be analyzed to provide maps of the line-of-sight and transverse magnetic fields and also a photospheric sunspot image of the active region. The magnetograph has a 6'.9 × 6'.9 field of view, which is larger than most active regions. The spatial resolution of the magnetograph is set by the 3".2 pixel size.

The *Yohkoh* SXT (Tsuneta et al. 1991) observes the coronal X-ray emission using 5 X-ray filters with different temperature response functions. A co-aligned telescope provides photospheric sunspot images. For this study, we used X-ray images obtained with the thin aluminum filter, which had the most extensive time coverage during our periods of interest.

Because we needed to co-align *Yohkoh* SXT X-ray images and MSFC vector magnetograms, we restricted our study

to the period of *Yohkoh* operation before 1992 November 13, after which *Yohkoh* lost the ability to produce photospheric sunspot images. We selected five active regions (Table 1) that had neutral lines with strong magnetic shear and that were well observed by the *Yohkoh* SXT and the MSFC magnetograph. Two of these active regions are the active regions examined by Moore et al. (1994) and Porter et al. (1994). For all our active regions except Active Region 6982, MSFC magnetograms were taken on multiple days. Nine magnetograms covering the five active regions were selected, each from a different day and representing the best observing conditions for that day.

For each of the selected magnetograms, we examined SXT thin aluminum filter images from three different orbits, which allowed us to determine what is typical and what is exceptional behavior, and what variations in enhanced coronal heating can occur on timescales of hours. Whenever possible, we analyzed images from the orbit before, during and after the time when the magnetogram was taken. Sometimes, for one reason or another, images from an orbit were not available for analysis. In this case, images from another orbit as close as possible to the time of the MSFC magnetogram were chosen. The start times of the orbits analyzed are given in Table 1.

### 2.2. *Maps of Neutral-Line Magnetic Shear*

In order to examine the relationship between neutral-line magnetic shear and enhanced coronal heating, we first identified the sites of such shear. This procedure involved setting some observational thresholds and finding a convenient representation for the quantity of shear, which must be derived from the vector magnetograms. We will use, as an example, the magnetogram of AR 6982 (the southwestern active region in Fig. 1), taken at 18:23 UT on 1991 December 26.

The magnetic shear is defined as the acute angle between the observed and potential transverse field. The potential transverse magnetic field (Fig. 2, *upper right*) was computed from the observed line-of-sight magnetic field (Teuber, Tandberg-Hanssen, & Hagyard 1977). We identified the nonpotential regions by superimposing the observed and potential magnetic field (Fig. 2, *lower left*). When the transverse field is weak, there is large uncertainty in its orientation, so the magnetic shear is not well determined. For the MSFC magnetograph, the 1 $\sigma$ uncertainty of the magnetic field strength for weak field regions ($|B| < 200$ G) is 50 G for line-of-sight magnetic field and 75 G for transverse field (Gary et al. 1987). So, for measuring the shear angle, we adopted 150 G as the threshold strength for both the observed and potential transverse fields. At transverse field strengths above this threshold, the uncertainty in the measured shear angle is less than about 10°.

To facilitate determining the sites of neutral-line magnetic shear, we have devised a neutral-line shear map. An example of such a map is shown at the lower right of Figure 2. Such a map highlights a neutral line and indicates whether the field along it is strongly or weakly sheared. To produce the neutral-line shear map, the location of the neutral line was first determined from the change of sign of the line-of-sight magnetic field. The degree of shear was then determined for the pixels that touched the neutral line and had transverse fields greater than 150 G by finding the acute angle between the observed and potential transverse field. Normally the "neutral lines" (i.e., the group of pixels selected above) in the neutral-line shear map are two pixels wide. Sometimes (usually at the end of a line) a short segment of a neutral line is only one pixel wide because the transverse field is less than 150 G for the pixels on the other side of the neutral line.

For this paper, we divide the degree of shear into only two classes: weak (less than 45°) and strong (greater than 45°) shear. We initially looked at finer divisions, but found that the relationship between neutral line shear strength and enhanced coronal heating was clearest when only these two classes were used.

### 2.3. *Criteria for Persistent Enhanced Coronal Heating*

Sequences of SXT images, such as those from AR 6982 taken on 1991 December 26 (Fig. 3, *bottom*) show intensity variation in the corona from flares, microflares, and more gradual changes of intensity of loops. While substructures within a site of enhanced coronal heating often change noticeably in brightness and form in a few minutes (Shimizu et al. 1992; Moore et al. 1994), the site as a whole usually continues to be outstandingly bright for several orbits. For the present investigation, we are interested in coronal fea-

TABLE 1

OBSERVATIONS

| AR Designation[a] | Date | Heliographic Location | | *Yohkoh* Orbit Times (Sunrise UT) | | | Magnetogram Observation Times (UT) |
|---|---|---|---|---|---|---|---|
| | | North-South[b] (deg) | East-West[c] (deg) | Orbit 1 | Orbit 2 | Orbit 3 | |
| 6982 ..... | 1991 Dec 26 | −10 | −20 | 17:58 | 21:13 | 2:06[d] | 15:43, 18:23 |
| 7070 ..... | 1992 Feb 27 | 8 | 2 | 8:40 | 17:50 | 19:28 | 15:10 |
| 7070 ..... | 1992 Feb 28 | 8 | −13 | 11:43 | 13:21 | 14:59 | 14:54 |
| 7220, 22 ..... | 1992 Jul 11 | −12 | 11 | 11:47 | 13:24 | 15:02 | 13:39 |
| 7220, 22 ..... | 1992 Jul 12 | −12 | −2 | 10:31 | 12:08 | 13:46 | 13:33 |
| 7260 ..... | 1992 Aug 16 | 17 | 28 | 13:40 | 15:18 | 16:55 | 15:26 |
| 7315 ..... | 1992 Oct 19 | 5 | 25 | 12:34 | 15:48 | 17:25 | 14:58 |
| 7315 ..... | 1992 Oct 21 | 5 | 6 | 13:15 | 14:54 | 16:31 | 15:25 |
| 7315 ..... | 1992 Oct 23 | 5 | −21 | 10:44 | 12:22 | 13:59 | 13:34 |

[a] From Sol.-Geophys. Data (1992).
[b] A positive value indicates north.
[c] A positive value indicates east.
[d] The third orbit analyzed was from the morning of 27 December 1991.

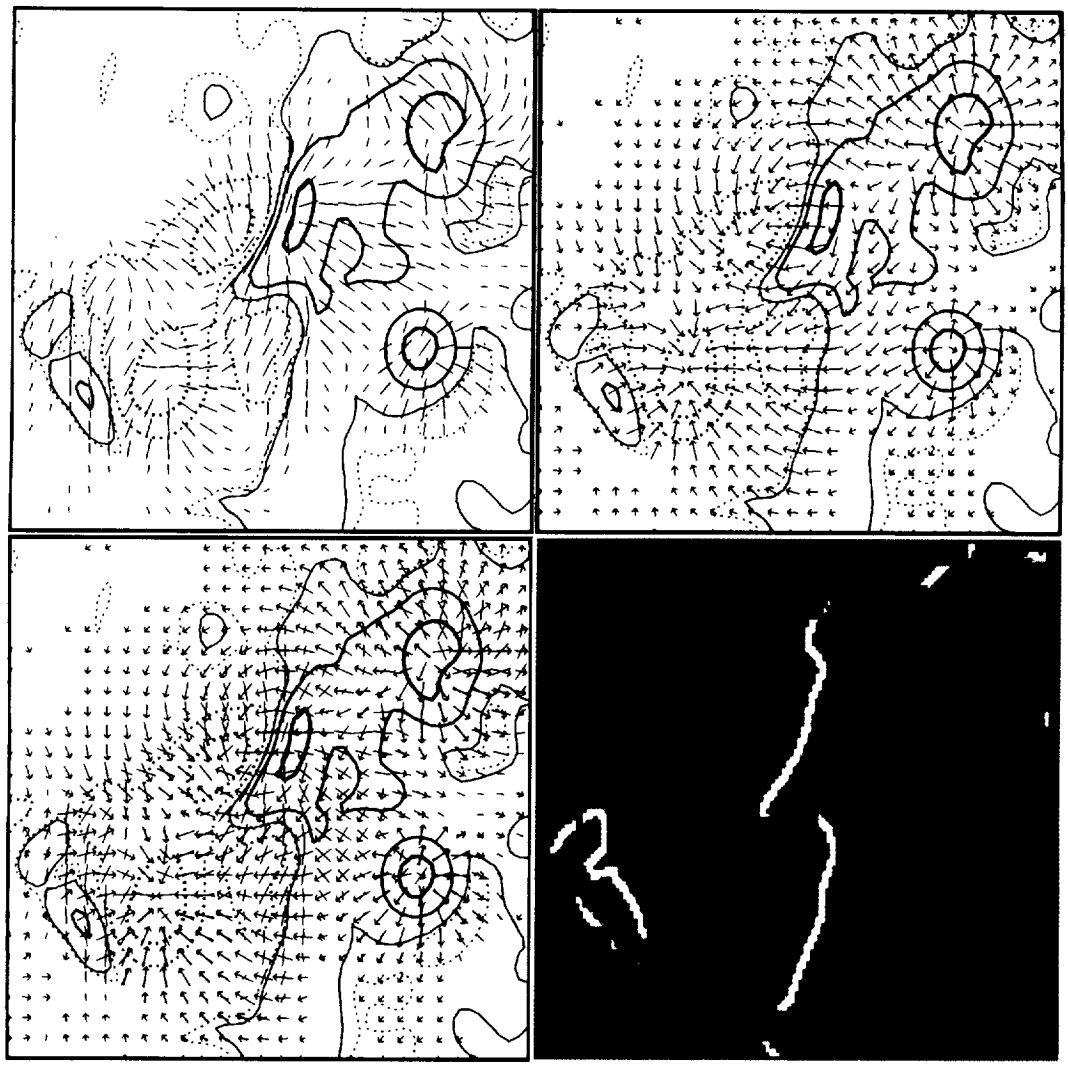

FIG. 2.—Mapping the nonpotentiality of an active region's core magnetic fields. *Top left*: MSFC vector magnetogram of AR 6982, the conspicuous active region southwest of disk center in Fig. 1, taken at 18:23 UT on 1991 December 26. North is up, west is to the right. The strength of the line-of-sight field component is mapped by the contours (*solid lines*, positive polarity; *dotted lines*, negative polarity; 25, 500, and 1500 G levels). The strength and orientation of the transverse field component is shown by the length and orientation of the dashes wherever this component is stronger than 150 G; the shortest dashes are for 150 G, the longest for 500 G or more. The 150 G lower bound keeps the error in the observed orientation less than about 10° on neutral lines. *Top right*: Potential transverse field computed from the observed line-of-sight field. Here and in the previous panel, for ease of viewing, the transverse field vectors are displayed for only one-fourth of the magnetogram pixels. *Bottom left*: The potential transverse field superposed on the observed transverse field. The greater the magnetic shear angle (defined as the acute angle between the observed transverse field and the potential transverse field), the greater the nonpotentiality of the observed field. It is evident that the field deviates most from the potential field along parts of the main neutral line and on the west side of the island of positive polarity in the negative domain of this overall bipolar active region. *Bottom right*: Neutral-line magnetic shear map. This map displays only those neutral-line segments on which the shear angle of the field can be accurately determined; that is, on which both the observed and the potential transverse fields are above our threshold of 150 G. The magnetic shear is strong (shear angle greater than 45°) in the white segments of the neutral lines and weak (shear angle less than 45°) in the gray segments.

tures that are persistently bright over the part of the orbit during which the active region is observed by *Yohkoh* (typically 30–50 minutes). We identified these features by constructing images of "persistent brightness" as follows. (1) The *Yohkoh* images from an orbit were co-aligned with each other. (2) The intensity of each image was normalized by the exposure time. (3) The minimum intensity measured for each pixel over the single-orbit observation time was determined. (4) The "persistent-brightness" coronal image (Fig. 3) was then constructed using the minimum intensity for each pixel.

Figure 3 shows many features that remained bright for at least 47 minutes. Since this time is longer than the cooling time for typical active-region coronal loops (Kano & Tsuneta 1995), these loops were apparently heated during the time of the observations. This heating might have been steady, episodic, or some combination of the two.

To examine the sites of enhanced coronal heating consistently, we had to set a minimum intensity threshold. Persistently bright coronal features have a wide range of brightness, up to about 10,000 DN $s^{-1}$. Because a brightness of 1000 DN $s^{-1}$ is just sufficient to identify a distinct bright feature and its footpoints, we chose 1000 DN $s^{-1}$ (per 2.″45 pixel) as the threshold. For emitting plasma at a temperature of (3–5) $\times$ $10^6$ K, the emission measure corresponding to 1000 DN $s^{-1}$ is roughly $3 \times 10^{44}$ $cm^{-3}$ (Tsuneta et al. 1991), where 1 DN $s^{-1}$ = $5.8 \times 10^{-10}$ ergs $s^{-1}$ at the SXT focal plane.

For this study, all the features from any one of the 27 orbits were counted independently of the features from all

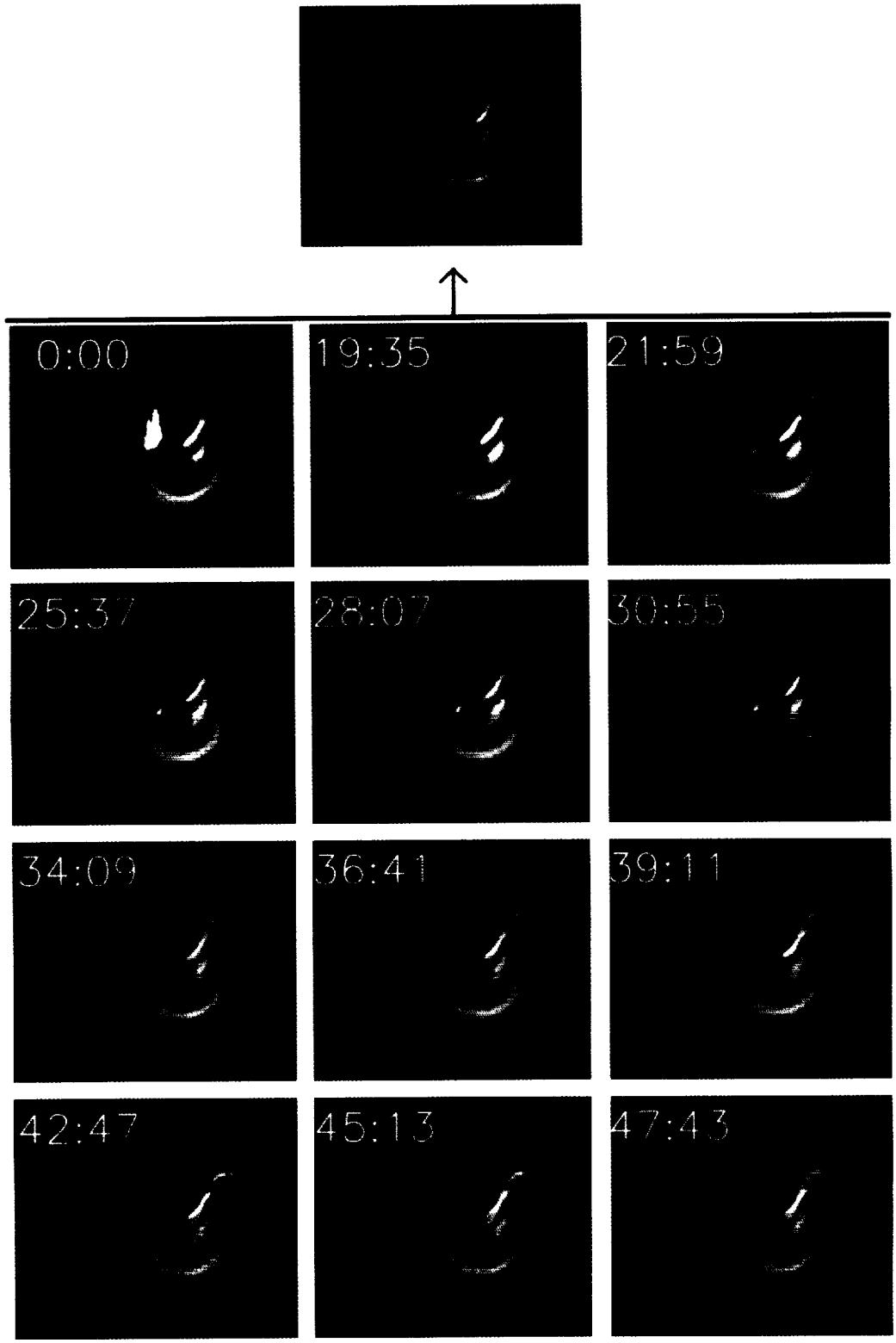


FIG. 3.—Selection of persistently strongly heated coronal features. *Bottom 12 panels*: SXT images showing the coronal brightness structure of the active region in Fig. 2 during the orbit that covered the time of the magnetogram in Fig. 2. For this orbit, these are all the images of this active region taken in Partial Frame mode with the thin aluminum filter and exposures of 338 or 168 ms; these images bring out the structure of the region's bright interior, and cover the full time span of the images from this orbit. Each frame is labeled with its time lapse from the first frame. It appears that the overall structure and most substructures persisted through the orbit, but that many of the substructures underwent various changes in brightness. All frames have been normalized to the same brightness scale to remove apparent brightness changes caused by changes in exposure time. *Top*: Composite image showing those features that were persistently bright throughout the orbit. This image was constructed from the lower 12 frames (except the two incomplete frames) by taking the minimum brightness for each pixel. Bright features mark sites where enhanced coronal heating persisted over this orbit. In the whitest areas, the brightness exceeds 3000 DN $s^{-1}$. In this paper, we limit our attention to coronal features that had a persistent brightness of at least 1000 DN $s^{-1}$ over an orbit.

the other orbits. Consequently, any feature that persisted over more than one of the three orbits selected for each day was counted two or three times. This procedure was adopted because the features that persisted for more than one orbit often changed shape from orbit to orbit, so that we thought it probable that different structures were being activated.

### 2.4. *Magnetic Location of Persistent Enhanced Coronal Heating*

In the previous two sections, we have described the neutral-line shear map and the persistent-brightness coronal image of an active region. Now we will combine the two.

Both the *Yohkoh* SXT and the MSFC magnetograph take photospheric sunspot images that are co-aligned with the other observations made by the same instrument. Hence we were able to co-align the *Yohkoh* SXT X-ray images and the MSFC magnetograms by co-aligning their sunspot images. The alignment was done interactively at a computer workstation. First the spatial scale of the MSFC image was adjusted to be the same as the SXT image. We then rotated and shifted the MSFC sunspot image so that the sunspots were co-aligned. The resulting co-alignment was normally accurate to a *Yohkoh* SXT pixel (2.″45) depending on the number and position of sunspots in the sunspot image. The co-alignment determined from sunspot images was then used to align the neutral-line shear map and the *Yohkoh* persistent brightness image, as shown in Figure 4. The superposition of the persistent brightness coronal image on the neutral-line shear map of an active region brings out the location of the enhanced coronal features relative to the neutral lines in the region and the degree of shear in the core fields along the neutral lines. This representation allows us to obtain statistics from different regions accurately and consistently.

Note how the brightest features in Figure 4 either follow the strong-shear neutral lines or have one end near the strong-shear neutral lines. Also, all of the long (longer than 25″) segments of the strong-shear neutral lines have enhanced coronal features along them, or have nearby footpoints of enhanced coronal loops, or both. The two long neutral lines with only weak shear do not have enhanced coronal features on or near them. The relationship between neutral-line shear and enhanced coronal heating suggested by Figure 4 is examined in detail in the next section.

## 3. RESULTS

### 3.1. *Enhanced Coronal Heating as a Marker of Strong Neutral-Line Magnetic Shear*

By examining the relationship between enhanced coronal heating and neutral line magnetic shear, we found four distinct categories of persistently bright coronal features. We also found that the various types of features differed in their affinity for neutral-lines with strong shear near their footpoints. All of our persistently bright coronal features were

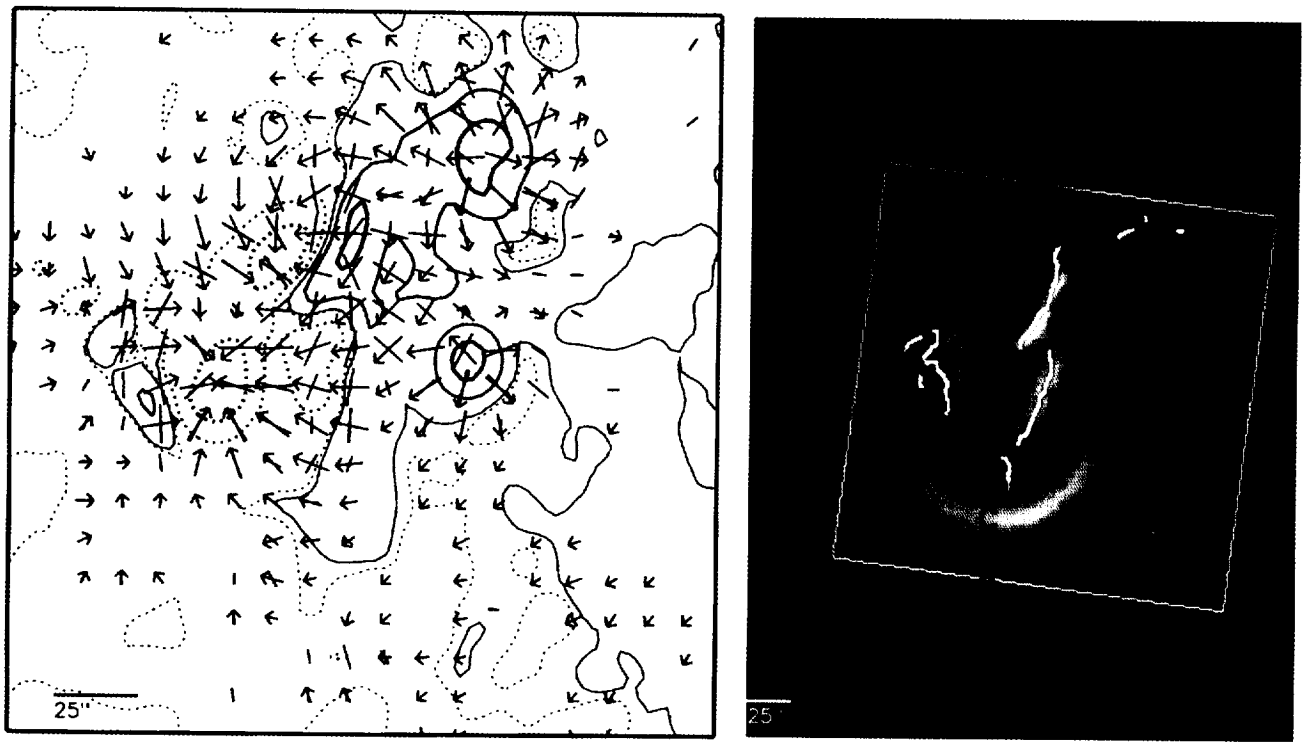


FIG. 4.—Location of strong coronal heating with respect to neutral-line magnetic shear. *Left*: Superposition of the same observed and potential vector magnetograms as in Fig. 2, but with a larger field of view showing more of the outskirts of the active region. It is seen that in the added area there is little transverse magnetic field above our 150 G threshold. In this display we have made the size and spacing of the transverse vectors twice those in Fig. 2. *Right*: The persistent-brightness coronal image from Fig. 3 superposed on the neutral-line magnetic shear map derived from the vector magnetogram in the left panel. The tilted square is the field of view of the left panel. The letters label conspicuous coronal features that are brighter than 1000 DN $s^{-1}$. We call features A, B, F, and G core features because each resides entirely in the core magnetic field closely enveloping a neutral line. Each of these four bright core features is centered on a segment of strong neutral-line magnetic shear. We call features C, D, and E extended loops because each has an end rooted near a neutral line and extends away from that neutral line. C and D stem from near the strong-shear neutral line that runs through F and G; E has one end near the strong-shear neutral line through A and has its other end near a strong-shear segment of another neutral line. The close linkages between enhanced coronal heating and neutral-line magnetic shear displayed here by this active region are typical of the five active regions we have studied.

seen to link opposite polarities across our strong-field neutral lines; that is, each overlapped or overarched at least one of our shear-map neutral lines, along which the field strength was greater than 150 G. The channels of strong magnetic shear along neutral lines were no wider than about 25″ (or about 20,000 km) in our active regions. Consequently, the length 25″ and half this length, 12″, are useful discriminators for sorting our bright coronal features into the four categories. The locations of the footpoints of coronal loops were determined using the apparent ends of the loops. Uncertainty in the location arises from the fact that the feet of the loops are cool, so that they are not readily visible in X-rays, and from projection effects, e.g., the leg of the loop can curve back so that the footpoint is covered by the body of the loop. For these reasons, we assume that the foot of a loop is rooted near a neutral line if the apparent foot is within 12″ of the neutral line.

A total of 94 different persistent bright X-ray features were identified and categorized. For this sample, the total population in each of the four categories is given in the bottom row of Table 2. In the order of frequency of occurrence, the four categories are defined as follows.

*Extended loops* (*Fig. 5, top left*).—To qualify for this category, a feature must look like a loop (i.e., be elongated), be longer than 25″, have at least one end near a neutral line (within 12″), and have some extent well away from any neutral line (beyond 12″). In Figure 5, loops B and D have only one end near a neutral line; A has one end near one neutral line, its other end near another neutral line, and its middle far from any neutral line; C has both ends near the same neutral line, but its middle is not near any neutral line. Our extended loops often stem from core features (defined next), as loop D does from core point E.

*Core features* (*Fig. 5, top right*).—To qualify for this category, a feature must sit on a neutral line and be closely confined to the neutral line (within 12″). Core features that are longer than 25″ along the neutral line we call core arcades; those shorter than 25″ we call core points. Features F and G in Figure 5 are core arcades; features E and H are core points.

*Forests of loops* (*Fig. 5, bottom left*).—These features cover parts of one or more neutral lines, have parts that extend far (more than 12″) from any neutral line, and are more complex than either an extended loop or a core feature alone. They appear to consist of core features and extended loops jumbled together.

*Isolated loops* (*Fig. 5, bottom right*).—To qualify for this category, a feature must look like a loop, be longer than 25″, and have each end farther than 12″ from any neutral line.

Figures 4, 6, 7, and 8 show examples of extended loops. The fields of extended loops appear to be closer to a potential field than the fields of core features are. Some extended loops have opposite footpoints near different neutral lines, e.g., feature E in Figure 4.

There are examples of core arcades in Figures 4 and 6 and examples of core points in Figures 4 and 8. Either core arcades (Figs. 4 and 6) or core points (Figs. 4 and 8) may have extended loops stemming from them. Core features, while persistently bright, fluctuate more in intensity than extended loops, as can be seen in Figure 3.

A forest of loops appears prominently in Figure 7 and less prominently in Figure 8. Extended loops may also be rooted in forests of loops, as in the case of extended loop B in Figure 7. In fact, if no clear separation had existed in this case, the forest of loops would have been thought to cover a larger area. It appears that a forest of loops is a combination of loops, the individual loops being obscured by overlapping. For example, the forest of loops in Figure 7 might be a combination of a core arcade and one or more extended loops.

An isolated loop does not have a neutral line near (i.e., closer than 12″ to) either footpoint, but of course it must cross a neutral line somewhere to be considered a loop. Our best example of this type of loop is feature C in Figure 8. A loop of this type appeared in this vicinity for two consecutive days. Both footpoints appear to be rooted in local maxima of strong (more than 500 G) unipolar flux. These two days of observations of this active region gave our only identifications of isolated loops. Isolated loops are by far the rarest of the four categories of features identified in this study.

So far, the degree of shear along neutral lines associated with coronal bright features has not been discussed. In Table 2, we give the incidence of strong or weak neutral-line magnetic shear near the footpoints of extended loops, core features, and forests of loops. For extended loops, if both footpoints were near a neutral line we assigned the higher degree of shear to the loop. For core arcades, the degree of shear along the majority of the arcade was assigned to the whole arcade. For forests of loops, as for extended loops, if the structure was rooted along two neutral lines we assigned the stronger shear. Isolated loops, by definition, have no neutral lines near their feet; hence, in Table 2, they have no assigned neutral-line magnetic shear strength. However, each of the isolated loops in our sample arched over a neutral line having weak magnetic shear.

From Table 2, we see that approximately 75% of the extended loops (35 out of 46) and forests of loops (9 of 12) have neutral-lines with predominantly strong shear near their feet. Throughout this paper we round the percentages to the nearest 5% because of our sample size, but we also give the exact count ratio from our sample in parentheses. In Table 2, note the high incidence of extended loops; about half the features observed (46 of 94) were extended loops. This number might, in fact, be an undercount, because most forests of loops probably contain at least one extended loop, and also because our survey may be biased, since it contains active regions with more strong-shear neutral lines than average and hence more core features than average.

Core features are even more likely than extended loops or forests of loops to be found on strong-shear rather than weak-shear neutral lines. All the core points were on strong-shear neutral lines, while 95% (20 of 21) of the core arcades were. The single exception had a short segment of high-shear neutral line near one end and its coronal brightness was just above threshold. During the next two orbits it was

TABLE 2

NEUTRAL-LINE MAGNETIC SHEAR NEAR FOOTPOINTS OF PERSISTENTLY BRIGHT CORONAL FEATURES

| | Types of Bright Features | | | | |
|---|---|---|---|---|---|
| Shear Strength | Extended Loops | Core Arcades | Core Points | Forest of Loops | Isolated Loops |
| Weak (<45°)..... | 11 | 1 | 0 | 3 | ... |
| Strong (>45°)..... | 35 | 20 | 11 | 9 | ... |
| Total ..... | 46 | 21 | 11 | 12 | 4 |

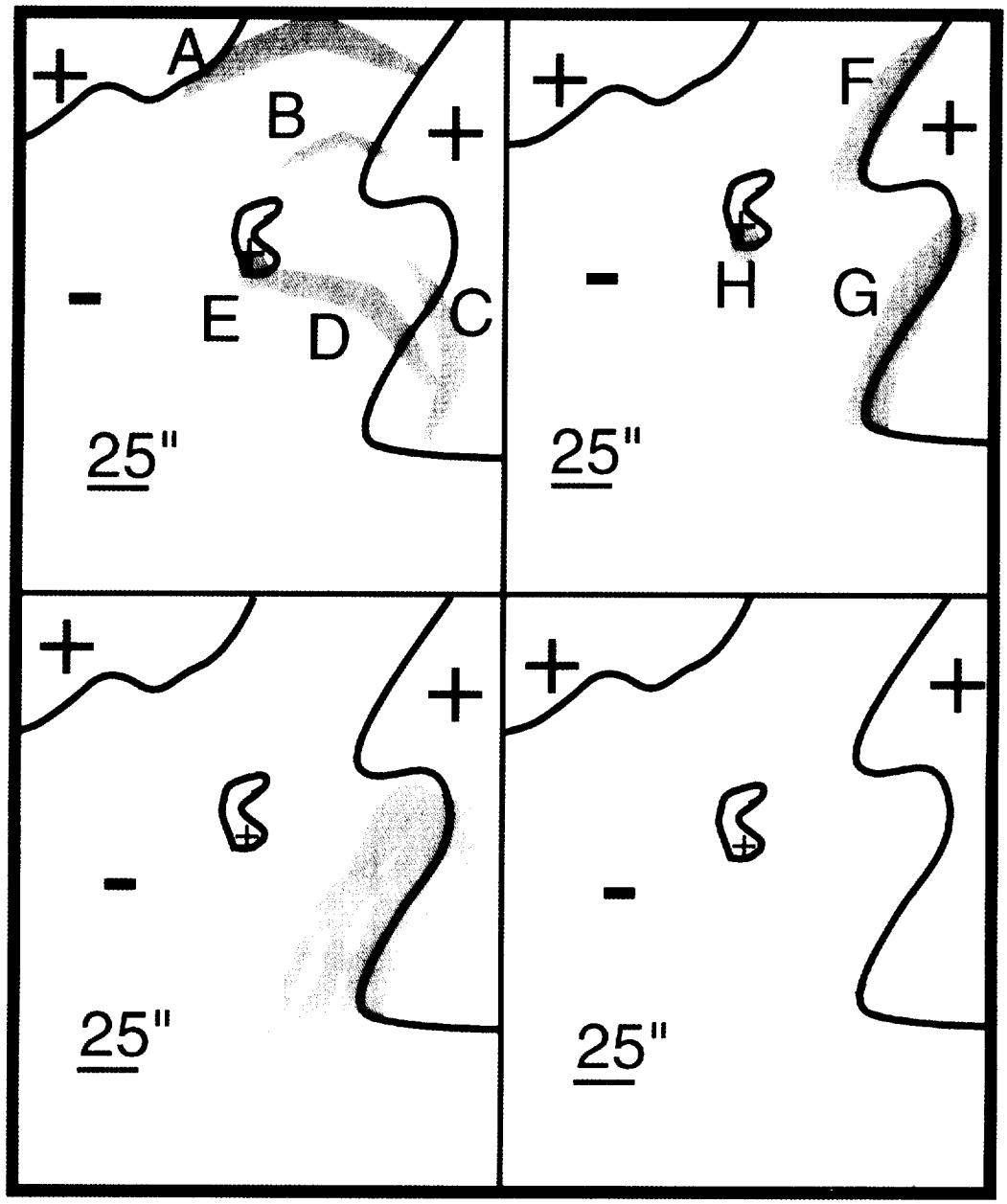


FIG. 5.—Sketches illustrating the four categories of persistently bright coronal features found in our set of active regions. Each panel illustrates the defining characteristics (see text) for one category by showing persistently bright coronal features (*gray*) superposed on the map of the neutral lines (*black*) in a hypothetical typical active region, a composite drawn from all of the active regions in the study. Each panel is analogous to the right panel of Fig. 4, except that the strength of neutral-line magnetic shear is not indicated. The magnetic polarity on either side of each neutral line is indicated by a plus sign or a minus sign. *Top left*: Extended loops. *Top right*: Core features. *Bottom left*: Forest of loops. *Bottom right*: Isolated loop.

too faint too be counted. Hence heating of core features is more likely or stronger on strong-shear neutral lines than on weak-shear neutral lines.

It should be noted that all features that were brighter than our minimum brightness threshold (1000 DN $s^{-1}$) had at least one footpoint in regions of magnetic field stronger than 150 G. We independently chose 150 G as our field strength threshold for reliable measurement of the magnetic shear on neutral lines. It turned out that the magnetic field strength also had to exceed this threshold for the persistent enhanced coronal heating mechanism to heat features to brighter than 1000 DN $s^{-1}$.

For about a third of all the persistent features, a sizable fraction of the feature area was brighter than 3000 DN $s^{-1}$. About 90% of these features were rooted near strong-shear neutral lines while only 80% (75 of 94) of all features were. Hence we find that more features and brighter features are rooted near strong-shear neutral lines than near weak-shear neutral lines.

### 3.2. *Strong Neutral-Line Magnetic Shear as a Marker of Enhanced Coronal Heating*

Next we assess whether neutral-line shear is a reliable marker of enhanced coronal heating. We want to look for enhanced coronal brightness near long segments (longer than 25″) of neutral lines with either purely weak or purely strong shear. This procedure allows us to investigate clear examples of both types of neutral lines and avoid neutral lines with mixed shear. For each long neutral-line segment, we determined if any bright feature was rooted near the

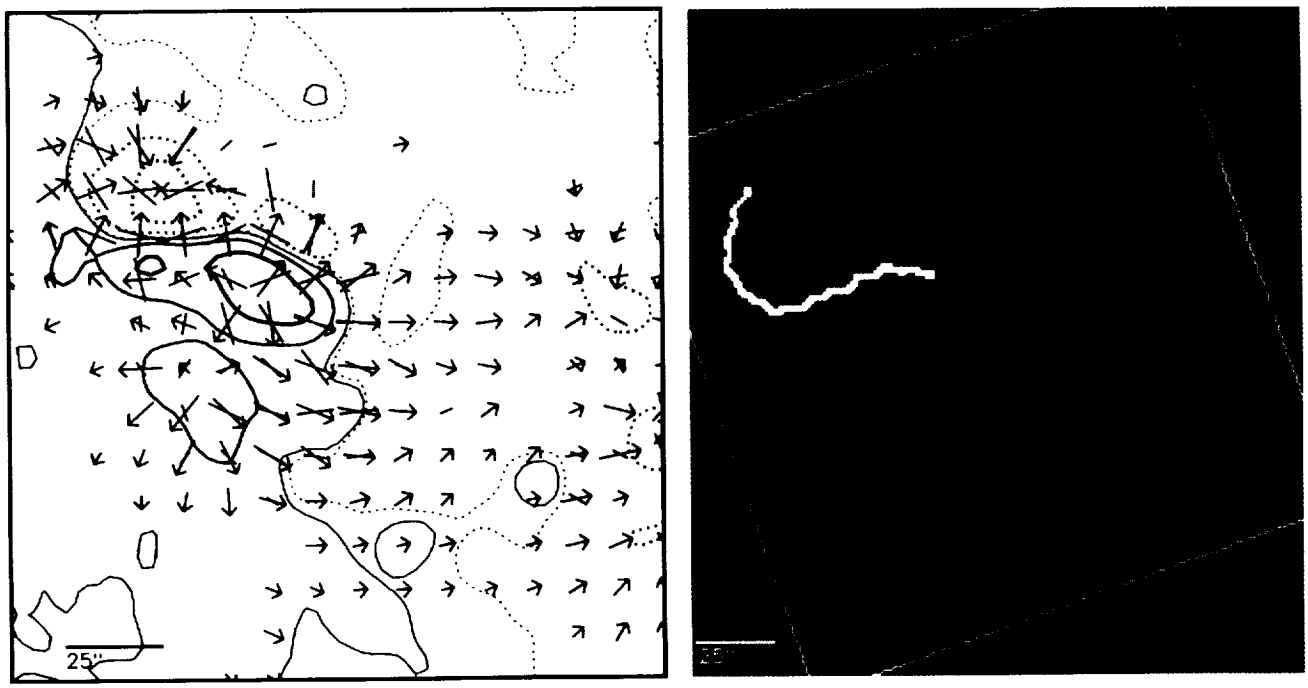


FIG. 6.—Same as Fig. 4, but for AR 7070 during the orbit with sunrise at 13:21 UT on 1992 February 28. Feature A is a strongly-sheared core arcade; B is an extended loop rooted near a strong-shear part of the neutral line; C and D are extended loops rooted near weak-shear parts of the neutral line. The faintest of these four features, extended loop D, is barely brighter than our brightness threshold; its brightest few pixels are 1000 DN $s^{-1}$. This active region had a simpler magnetic field configuration and dimmer enhanced coronal features than the active region in Fig. 4.

segment, and, if so, what type of feature it was. If there was a post-flare loop above the neutral line, or the neutral line was near the edge of the *Yohkoh* image or magnetogram so that it was not possible to classify the nearby enhanced coronal bright features, the neutral line was not included in the survey. The incidence of each type of enhanced bright feature with neutral-line segments of all strong or all weak magnetic shear is listed in Table 3.

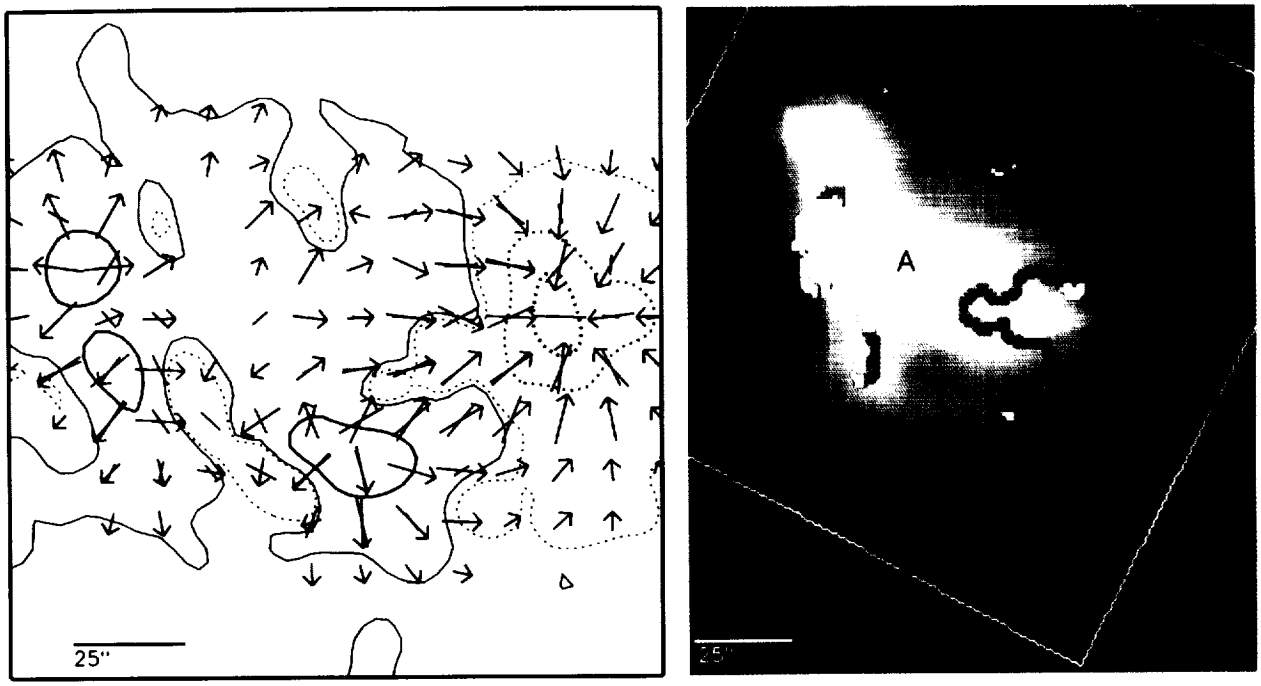


FIG. 7.—Same as Fig. 4, but for AR 7315 during the orbit with sunrise at 17:25 UT on 1992 October 19. Gray-scale saturation in this figure due to the uniform intensity scale used throughout this paper exaggerates the problem of determining the structures within Feature A, but even in an image with no saturation, the overlapping of many structures in this area makes it impossible to determine the exact number or types of loops it consists of, resulting in its classification as a forest of loops. Feature A covers all of one neutral line (the one seen to be peanut-shaped in the magnetogram) and much of another. Much of the completely covered neutral line has strong magnetic shear; the partially covered one has predominantly weak magnetic shear. Between these two neutral lines, in the northern half of the area covered by the forest of coronal loops, the observed photospheric magnetic field is nearly a potential field. Feature B is an extended loop with one end near the strong-shear neutral line and its other end in a nearly potential field and far from any neutral line. These observations suggest that the enhanced coronal heating in both A and B was a consequence of their being rooted near strong neutral-line magnetic shear.

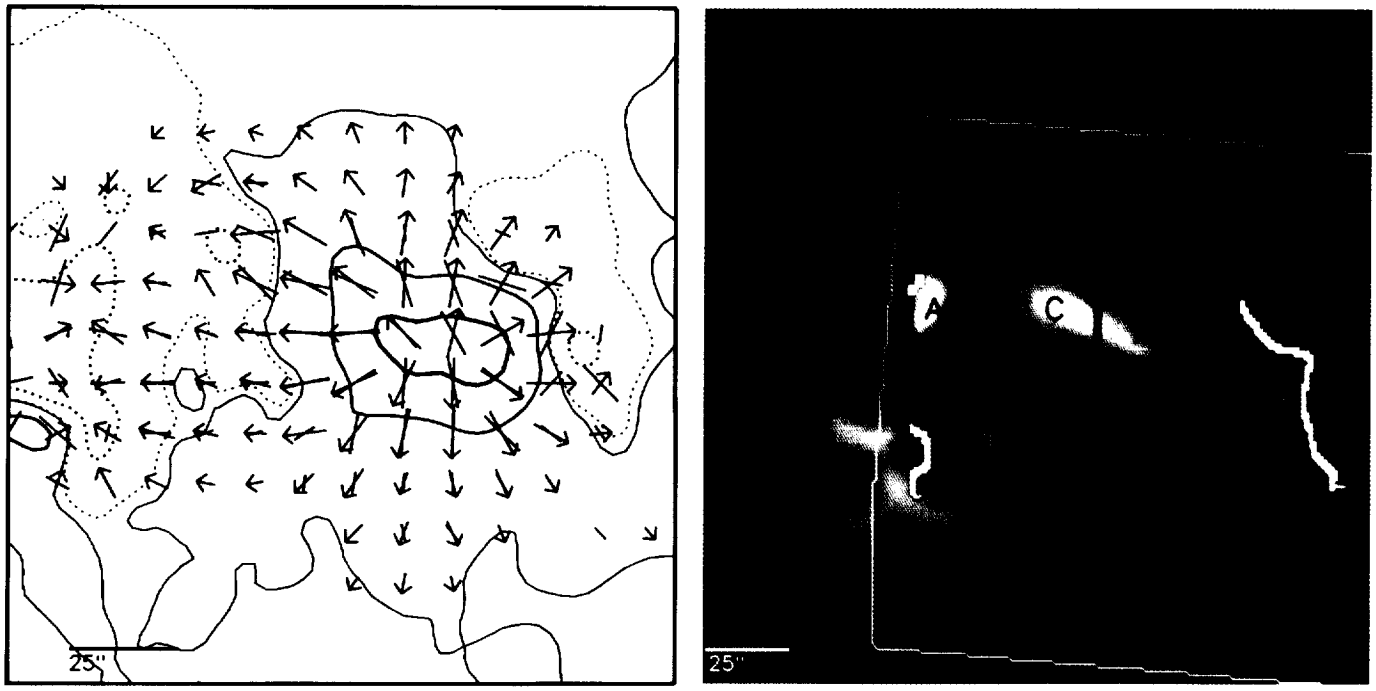


FIG. 8.—Same as Fig. 4, but for AR 7222 during the orbit with sunrise at 10:31 UT on 1992 July 12. Feature A is a core point partly over the strong-shear part of the neutral line around a small island of included polarity that was barely detectable by the magnetograph. Feature B is an extended loop that extends from near the same strong-shear neutral line, arches over a long neutral line of weak magnetic shear, and comes down in nearly potential field far from any neutral line. Feature C is a clear example of an isolated loop; each end is far from any observed neutral line. We found only four isolated loops; these all bridge this same weak-shear neutral line. Feature D is another extended loop; it extends from near a strong-shear neutral line, arches over the meandering weak-shear main neutral line of the overall bipole, and ends in the same large area of nearly potential positive field as B and C. Feature E is a forest of loops connected with the same strong-shear neutral line as D. Neutral line F is exceptional in that, even though it has strong magnetic shear all along it, it has no bright core features, only a dim core arcade too faint (less than 1000 DN $s^{-1}$) to qualify as one of our sites of strongly enhanced coronal heating.

The neutral-line segments with enhanced coronal features rooted on or near them were counted separately for each orbit. Thus, each neutral-line segment in an active region was usually counted three times, once for each of the three orbits. In Table 3 we give the numbers of weak-shear or strong-shear neutral-line segments, rather than the numbers of features, as in Table 2. Thus only 16 out of 39 weak-shear segments had some type of bright feature rooted near them, while only 6 out of 40 strong-shear segments had no bright features rooted near them.

From Table 3 we can determine the following facts. Strong-shear neutral lines are good markers of sites of enhanced coronal heating. Strong-shear neutral lines are more likely (85%; 34 of 40) to be near enhanced coronal brightness than weak-shear neutral lines (40%; 16 of 39). This disparity between strong-shear and weak-shear neutral lines is the most extreme for core features: no weak-shear neutral line had a core point and only one had a core arcade. The only type of feature that both strong and weak-shear neutral lines have roughly the same chance of having is extended loops.

Strong-shear neutral lines often have multiple features, while weak-shear neutral lines rarely do. Only one weak-shear neutral line had multiple features that were brighter

TABLE 3

INCIDENCE OF ENHANCED CORONAL HEATING NEAR LONG SEGMENTS OF STRONG OR WEAK NEUTRAL-LINE MAGNETIC SHEAR

| | | Type of Bright Features | | | | |
|---|---|---|---|---|---|---|
| Shear Strength | Number of Segments[a] | Extended Loops[b] | Core Arcades | Core Points | Forest of Loops[c] | Total |
| Weak (<45°)..... | 39 | 9 | 1 | 0 | 6 | 16 |
| Strong (>45°)..... | 40 | 11 | 17 | 6 | 11 | 34 |

NOTE.—Many strong-shear neutral-line segments had more than one type of bright feature rooted near them. Each of these segments was counted once for each type of bright feature that it had. Consequently, for the strong-shear neutral line segments, the sum of the counts under the four feature types (45) is greater than the number of strong-shear neutral-line segments having any type of bright feature (34) and even exceeds the total number of strong-shear neutral-line segments (40).

[a] Neutral-line segments with flares over them were not included in the survey while the flare persisted.

[b] When an extended loop had footpoints on two neutral-line segments, both segments were counted as having extended loops.

[c] When a forest of loops covered more than one neutral-line segment, all covered segments were counted as having a forest of loops (e.g., Fig. 7).

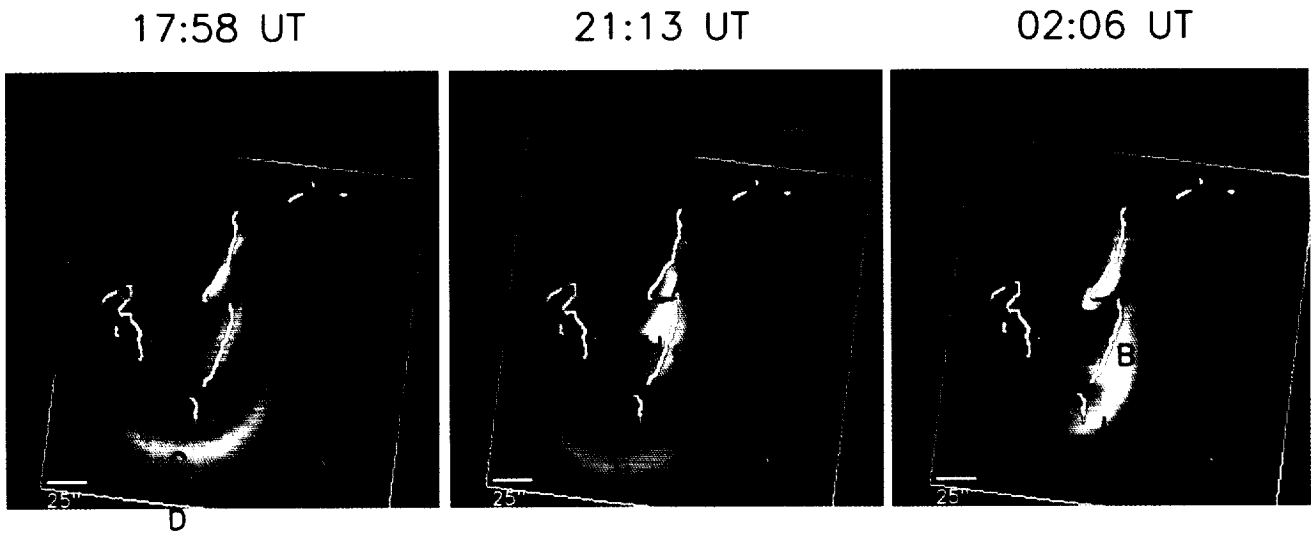


FIG. 9.—Changes in the persistently bright coronal structure of an active region over several hours. This sequence (together with Fig. 3) exemplifies that while enhanced coronal heating in active regions generally persists in the same places for about an hour, it often changes markedly in a few hours. *Left*: Persistent coronal brightness in AR 6982 (for the orbit with sunrise at 17:58 UT on 1991 December 26) superposed on the neutral-line magnetic shear map from the 18:23 UT magnetogram. Except for its smaller field of view, this frame is the same as the right panel of Fig. 4. *Middle*: Same as on the left, except that the persistent coronal brightness image is from the orbit with sunrise at 21:13 UT (two orbits later). *Right*: Same as on the left, except that the persistent brightness image is from the orbit with sunrise at 02:06 UT on December 27 (three orbits after the second frame and five orbits after the first frame). All of the bright features labeled by letters change in brightness or shape or both from frame to frame. Extended loop D is below threshold after the first frame; core point G and extended loop E are below threshold in the last frame. Extended loop E is obviously not the same magnetic loop in the first and second frames; extended loop C shifts southward in each successive frame. Core arcade H is seen only in the second frame; extended loop I is noticeable only in the last frame. All five of our active regions displayed comparably large orbit-to-orbit changes in their persistently bright coronal features.

than our minimum requirement, the one shown in Figure 6 with 2 extended loops, C and D. In the next orbit, C and D were both still visible and above threshold, and another bright loop extended westward from the weak-shear segment north of loop C. Since forests of loops may in reality consist of multiple extended loops, some of the forests of loops over the weak-shear neutral lines might be other examples of multiple extended loops rooted on weak-

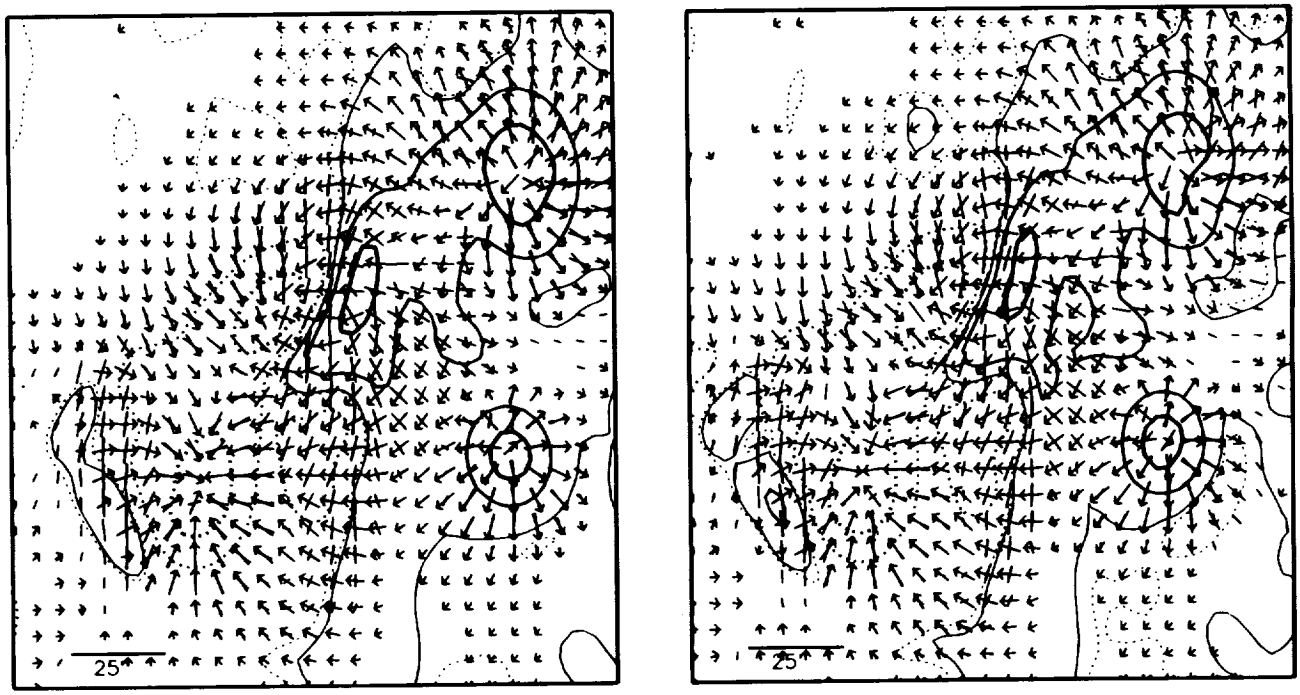

FIG. 10.—Constancy of an active region's magnetic field in the MSFC vector magnetograms. *Right*: Superposed observed and potential vector magnetograms of the active region in Fig. 9 at 18:23 UT on 1991 December 26. This panel is the same as the lower left panel of Fig. 2. *Left*: Superposed observed and potential vector magnetograms of the same region about 3 hr earlier. None of the changes between these two frames can be taken to be real; all changes are small and are plausibly due to the improvement in seeing that often occurs between 15:00 and 18:00 UT at the MSFC Solar Observatory. Even with sustained good seeing, MSFC vector magnetograms seldom show any significant changes in an active region's magnetic field over times of several hours or less. Thus, if any of the coronal brightness changes in Fig. 9 came from changes in the photospheric magnetic field, those changes were probably too small to be discerned in MSFC vector magnetograms.

shear neutral lines. Even so, less than 20% (no more than 7 of 39) of the weak-shear neutral lines could have had multiple extended loops.

A given degree of shear, however, does not always produce the same degree of brightness or type of bright coronal feature on or near a neutral line. In Figure 8, a clear example of a long strong-shear neutral line is shown but no enhanced coronal features were observed to be rooted on or near this neutral line; it was surrounded only by faint isolated haze. On the previous day it had only one core point on it. While some heating occurred to produce the isolated faint haze, the strength of the heating was much less than usual for a strong-shear neutral line.

Our survey might have a bias toward a higher incidence of strong-shear neutral lines than would be found in an average active region, because our active regions were selected to have at least one strong-shear neutral line. In an unbiased sample of active regions there would probably be more weak-shear neutral lines than strong-shear neutral lines, rather than the roughly equal numbers found in our sample. This bias would not affect the results in Table 3, though it might affect Table 2. If an "average" active region had more weak-shear neutral lines than the active regions in our survey, then the numbers of extended loops and forests of loops relative to core features would probably increase.

### 3.3. *Changes in Enhanced Coronal Heating with "Constant" Magnetic Roots*

The persistent-brightness coronal images of each active region change from orbit to orbit. In Figure 3, brightness variations within individual enhanced features are easily visible during an orbit, while, overall, the larger features persist throughout the orbit. In Figure 9, persistent brightness images from three different orbits are shown for our example active region of Figures 2, 3, and 4. Some loops disappear, while others turn on over a period of 6 hr; in these loops the degree of persistent enhanced coronal heating must change. What causes this change in enhanced coronal heating? If we examine two magnetograms taken 2 hr 40 minutes apart (Fig. 10), no significant variation between the two is detected that could not be explained by improved seeing and reduced wind during the second observation. Whatever turns the heating on or off is not detectable in our magnetograms. Still, the neutral-line magnetic shear is a clear marker of where heating is likely; this fact must be explained by any heating mechanism theory.

## 4. SUMMARY AND DISCUSSION

The *Yohkoh* SXT coronal X-ray images, like the coronal images from *Skylab*, plainly show that the brightness of the corona, and hence the strength of coronal heating, is generally much greater in regions of strong magnetic field (active regions) than in regions of weak magnetic field (quiet regions). This simple observation alone implies that coronal heating is a magnetic phenomenon. The SXT coronal images also show that within an active region there are localized sites where the coronal brightness is persistently noticeably brighter than in the rest of the active region. Given that coronal heating is a magnetic effect, it is reasonable to expect that these sites of enhanced coronal heating are places in the active region's magnetic field where the field has some structure not present elsewhere. In terms of practical observations, we might expect the bright coronal substructures in active regions to be rooted in places that stand out in some way in photospheric magnetograms. If so, the observed arrangement of the magnetic field at these sites might shed light on the coronal heating process. With this motivation, we have examined the magnetic structure at sites of enhanced coronal heating in active regions by superposing *Yohkoh* SXT coronal images on MSFC vector magnetograms.

At the outset of the present study, we already knew from a limited sample of only two active regions (each over only one *Yohkoh* orbit) that, at least in some active regions, during some orbits, most persistently bright coronal features are rooted near neutral lines with strong magnetic shear (Moore et al. 1994; Porter et al. 1994). This result led us, in the present expanded study of five active regions over a total of nine days and 27 orbits, to focus on the connection of enhanced coronal heating with strong neutral-line magnetic shear. Our minimum goal was to determine whether the two exploratory active regions were typical or exceptional in showing enhanced coronal heating to be closely linked with strongly sheared core magnetic fields. The answer is listed below as the second of six points summarizing our results. Most of these findings are depicted in Figure 11.

1. Within each of our active regions, during any one *Yohkoh* orbit, there were several noticeably enhanced coronal features that persisted throughout the typically 30–50 minute sequences of SXT coronal images. These enhanced features were typically 2–3 times brighter that the rest of the active region, together covered less than half of the active region, and were always rooted in magnetic fields stronger than 150 G.

2. The pronounced tendency for the enhanced coronal structures to be contiguous with strong neutral-line magnetic shear, previously found from exploration of only two active regions, proved to be typical: in the expanded sample a large majority (80%) of our strongly heated coronal structures were embedded in or rooted in strongly sheared core magnetic fields. Thus, enhanced coronal brightness is a reliable, but not infallible, indicator of strong neutral-line magnetic shear in the same part of the active region.

3. While only a small minority (20%) of our enhanced coronal features were not rooted near neutral lines with strong magnetic shear, a large majority (80%; 15 of 19) of this minority were rooted near neutral lines with weak magnetic shear. That is, nearly all (95%; 90 of 94) enhanced coronal features were rooted near neutral lines regardless of the degree of neutral-line magnetic shear; only a few (5%; 4 of 94) were isolated loops, not rooted near any detectable neutral line.

4. Of the segments of strong neutral-line magnetic shear longer than 20,000 km, a large majority (85%) had one or more enhanced coronal features rooted near them, but 15% did not. That is, to about the same degree that enhanced coronal heating is a reliable marker of strong neutral-line magnetic shear, strong neutral-line magnetic shear is a reliable marker of enhanced coronal heating. We emphasize that the expanded sample of the present study shows that the presence of strong neutral-line magnetic shear does not guarantee the presence of strong coronal heating. This finding is new; the exploratory sample of two active regions had no such exceptions.

5. Of the segments of weak neutral-line magnetic shear

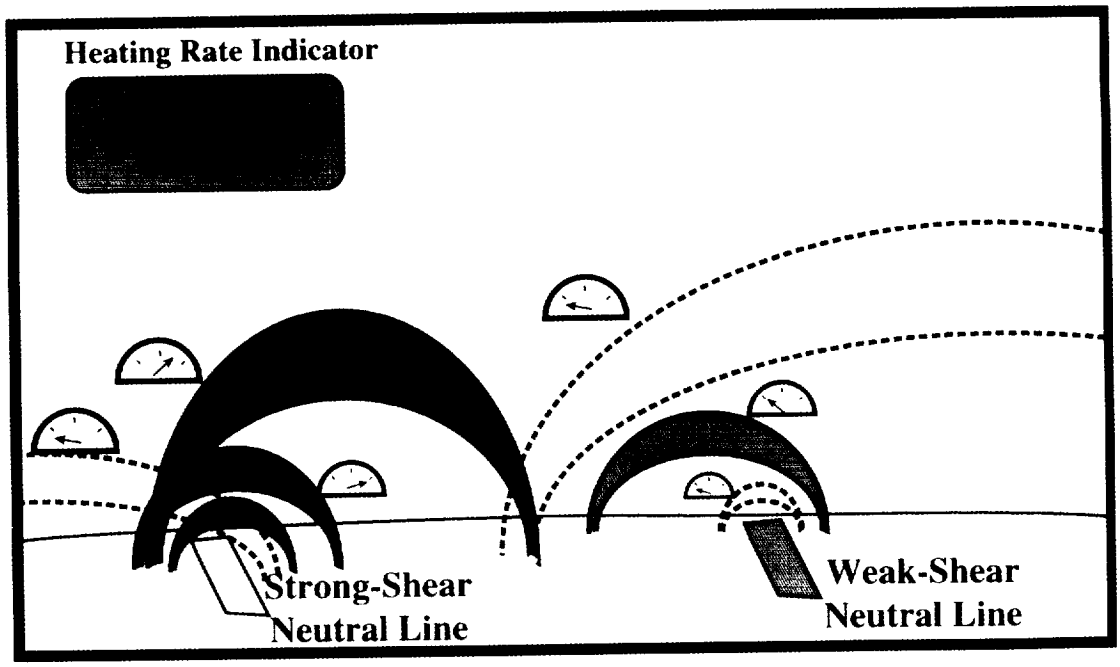


FIG. 11.—Cartoon summary of our findings as a sketch of an idealized active region viewed from the side and at a small angle above horizontal. There are two neutral lines viewed nearly end on, one with strong shear, the other with weak shear. The magnetic field of this active region fills the whole extent of the frame above the solar surface; only a few of the loops of this field are drawn. The shaded loops represent our persistently bright coronal loops, with deeper shading for greater brightness; the unshaded loops represent loops with persistent brightness below our threshold. To emphasize that enhanced coronal brightness requires enhanced coronal heating, the dial next to each loop indicates the heating rate per unit volume in that loop relative to the other loops. The sketch depicts that (1) only a small fraction of the total coronal volume of an active region's strong magnetic field is filled by coronal loops brighter than our threshold, (2) nearly all of these are rooted near neutral lines, (3) more bright loops are rooted near neutral lines with strong magnetic shear than are rooted near neutral lines with weak magnetic shear, and (4) different loops rooted near neutral lines with the same field strength and degree of shear can differ greatly in coronal brightness. These findings imply that the enhanced coronal heating in active regions is predominantly the result of some process that requires the presence of a neutral line and is more effective in the presence of strong magnetic shear in the core field along that neutral line, but also depends on some hidden variable agent or process. This hidden process, together with the strength and shear of the core magnetic field, determines the rate of heating (i.e., sets the dial).

longer than 20,000 km, a majority (60%) did not have enhanced coronal features rooted near them, but 40% did. That is, a neutral line without strong shear in the core magnetic field along it is an unreliable marker of strong coronal heating. On the other hand, weak-shear neutral lines are often populated with enhanced coronal features in the same way as for strong-shear neutral lines, but with the difference that the enhanced features rooted along weak-shear neutral lines are on average dimmer and sparser than those rooted along strong-shear neutral lines.

6. While all of our enhanced coronal features (by selection) persisted for the span of the SXT coronal images from one orbit, many of these features faded away or rose above threshold from orbit to orbit or over a few orbits. Over times this short, the magnetic flux and neutral-line magnetic shear in an active region usually remained constant within the accuracy of the MSFC vector magnetograms. That is, if the changes in enhanced coronal heating are caused by changes in the local magnetic structure (e.g., in the degree of neutral-line magnetic shear), these magnetic changes are probably too small to be detected by the MSFC magnetograph.

A study similar to ours was carried out by Webb & Zirin (1981). They compared *Skylab* coronal images with conventional magnetograms of active regions. They found that the brighter coronal loops often were rooted at satellite sunspots or sites of emerging magnetic flux near sunspots, places where the magnetic field was strong, changing, and of mixed polarity. Our study complements and extends the Webb & Zirin *Skylab* study by bringing together two improved data sets, namely the *Yohkoh* SXT images and the MSFC vector magnetograms of active regions. The *Yohkoh* SXT coronal images give us a sharper view of the brightest coronal structures in active regions, while the vector magnetograms allow us to more quantitatively gauge the nonpotentiality of the magnetic field where the coronal heating is strong. Our study confirms the Webb & Zirin finding that the brightest coronal loops are rooted in strong magnetic field of mixed polarity. In addition, we have established that the degree of nonpotentiality of the mixed-polarity magnetic roots (the neutral-line magnetic shear) is another key factor involved in strong coronal heating in active regions.

What do our empirical findings imply about the coronal heating mechanism or process in enhanced coronal features? First of all, the finding that nearly all enhanced coronal features are rooted near neutral lines suggests that the heating mechanism requires the presence of a neutral line in order to operate. If a neutral line is crucial for the heating in all cases for which a neutral line is observed in the magnetic roots of the enhanced coronal feature, then there are two possibilities for the heating in those few cases (the isolated loops) in which the feet are not near any neutral line seen in our magnetograms: either isolated loops are heated by a different mechanism from the one that heats other enhanced coronal features, one that operates without a neutral line near a foot, or else isolated loops are heated by the same mechanism that heats other features. The second possibility requires that a neutral line is present near at least one foot of each isolated loop but is not detected in

our magnetograms, as would be the case, e.g., for loop B in Figure 8 if the included polarity flux was somewhat smaller. Magnetograms with higher spatial resolution than ours will be necessary to distinguish between these two alternatives. In any case, our results suggest that enhanced coronal heating usually requires a polarity inversion in the magnetic roots of the enhanced coronal feature.

The finding that the large majority of enhanced coronal features have strong magnetic shear along neutral lines at their feet and the finding that a significant minority of enhanced coronal features have only weak magnetic shear along the neutral lines at their feet are both compatible with the assumption that the heating results from a process that acts only in the presence of a neutral line. Furthermore, these two findings together suggest the following two opposite possibilities for the role of sheared magnetic field in this process. One possibility is that the process taps the stored magnetic energy in the sheared core field to fuel the enhanced coronal heating. In this case, the process requires, in addition to a neutral line, the presence of magnetic shear in order to produce coronal heating, and is more effective in the presence of strong magnetic shear than in the presence of only weak magnetic shear. The opposite possibility is that the process produces coronal heating equally well with or without the presence of strong magnetic shear and does not tap the energy of the sheared magnetic field, but that it is involved in the production of shear in the field along the inversion line. In this case, the energy in the sheared core field is not the fuel for the enhanced coronal heating, but is only a passive by-product of the heating process that involves the neutral line. Either possibility is compatible with all of our empirical findings on the location of enhanced coronal heating with respect to neutral lines and neutral-line magnetic shear in active regions, except perhaps the tendency for the enhanced coronal features on or near strong-shear neutral lines to be brighter than those on or near weak-shear neutral lines. This tendency favors the idea that at least some of the energy for the enhanced heating comes from the sheared magnetic field.

Finally, we consider the finding that the heating of coronal structures rooted in sites having neutral line segments with the same field strength and the same degree of magnetic shear differs greatly from site to site or from orbit to orbit at the same site. This result suggests that while the heating process probably requires the presence of a neutral line, and may well be made more effective by the presence of strong magnetic shear, neither the presence of a neutral line nor the presence of strong magnetic shear forces the process to act or dictates the rate of the process. Apparently, the process can wax and wane while the local magnetic conditions remain constant to within the resolution of our vector magnetograph. If the process produces any change in the local field structure, for any typical hour-long heating episode these changes are too small to be seen in our observations. In this sense, our empirical results imply the presence of a hidden process that controls the rate of coronal heating (sets the dial in Fig. 11) in each neighborhood along a neutral line.

There is a well-known process that is compatible with, and hence is suggested by, the above clues for the process that controls the enhanced coronal heating: magnetic flux cancellation. Flux cancellation refers to the removal of magnetic flux from the photosphere by the merging of flux of opposite polarities (e.g., Zwaan 1987). Although flux cancellation can occur by the simple submergence of a magnetic loop (Rabin, Moore, & Hagyard 1984), in most cases it probably proceeds through reconnection of opposite polarity fields at or near the level of the photosphere. In any case, flux cancellation, by its very nature, requires the presence of a photospheric neutral line in order to occur. Flux cancellation appears to be mainly driven by convective flows (Zwaan 1987) carrying heat from below the photosphere. Cancellation may occur between pre-existing flux elements driven together by flows, or between emerging elements and the pre-existing flux elements as the new elements rise into them. Hence it is plausible that flux cancellation can start, stop, speed up, or slow down independently of the degree of magnetic shear at the neutral line. It has been observed that chromospheric microflaring is produced at sites of flux cancellation (Roy & Michalitsanos 1974; Martin, Livi, & Wang 1985). There is also evidence that flux cancellation can result in an increase in neutral-line magnetic shear (Martin 1986). Moore & Roumeliotis (1992) have proposed that flux cancellation can trigger sheared core fields to produce major flares by explosively erupting. Moore et al. (1994) have built on this idea to suggest that, in a similar way, flux cancellation can trigger localized microflares in sheared core fields. On the other hand, it may be possible that, instead of triggering microflares that draw their energy from the sheared field, flux cancellation drives microflares directly, through the driving of photospheric reconnection. Regardless of whether flux cancellation drives microflaring directly or triggers microflaring in sheared core fields or both, flux cancellation is a known process that acts only in the presence of a neutral line, probably can proceed independently of the degree of neutral-line magnetic shear, and is observed to occur with microflaring. As pointed out by Moore et al. (1994) and Porter et al. (1994), this microflaring might both directly heat the coronal plasma in the local core field and generate waves that propagate into extended loops and dissipate there to produce the enhanced coronal heating in the bodies of these larger structures.

In conclusion, we infer from our observations that magnetograms with substantially better spatial resolution, time resolution, and sensitivity than our present ground-based magnetograms will show a close synchrony between flux cancellation and enhanced coronal heating in active regions. This prediction might be testable with magnetograms from ground-based observatories during excellent seeing. A definitive test may well require magnetograms made in perfect seeing from above much or all of the Earth's atmosphere, on a high-altitude balloon or in orbit. A parallel question is the question of the magnetic origin of coronal heating in quiet regions. In particular, does neutral-line magnetic shear have an important role in the heating of the corona in quiet regions that is similar to its role in the strong coronal heating in active regions? The quiet-region core fields, covering the neutral lines that lace the mixed-polarity magnetic network, are numerous, but are of weaker field strength and of much smaller scale than the core fields along the major neutral lines in active regions. Consequently, observations of neutral-line magnetic shear in the magnetic network await more sensitive vector magnetographs and observing stations with much better seeing. However, by combining SOHO EUV Imaging Telescope (EIT) coronal images with conventional magnetograms from the SOHO Michelson Doppler Imager and/or ground-based

observatories, we plan to test whether coronal heating in quiet regions has mixed-polarity magnetic origins, as heating in active regions does.

We thank the following colleagues: Kathy Shearer for her initial work on the project, the scientists at *Yohkoh* and Lockheed for answering questions about *Yohkoh*, especially Samuel L. Freeland and Mons D. Morrison, and the scientists at the MSFC magnetograph, Mona Hagyard, Ed West, and James Smith, for help with the vector magnetograms used here. The paper was improved by many comments and suggestions from the referee. This work was funded by the Solar Physics Branch of NASA's Office of Space Science.

## REFERENCES

Ambastha, A., Hagyard, H. J., & West, E. A. 1993, Sol. Phys., 148, 277
Antiochos, S. K. 1990, J. Ital. Astron. Soc., 61, 369
Gary, G. A., Moore, R. L., Hagyard M. J., & Haisch, B. M. 1987, ApJ, 314, 782
Hagyard, M., Cumings, N. P., & West, E. A. 1985, in Proc. Kunming Workshop on Solar Physics and Interplanetary Traveling Phenomena, vol. 2, ed. C. de Jager & C. Biao (Beijing: Science Press), 1216
Hagyard, M., Cumings, N. P., West, E. A., & Smith, J. E. 1982, Sol. Phys., 80, 33
Hagyard, M., Smith, J. B., Teuber, D. L., & West, E. A. 1984, Sol. Phys., 91, 115
Kano, R., & Tsuneta, S. 1995, ApJ, 454, 934
———. 1996, PASJ, 48, 535
Kuperus, M., Ionson, J. A., & Spicer, D. S. 1981, ARA&A, 19, 7
Martin, S. F. 1986, in Coronal and Prominence Plasmas, ed. A. I. Poland (Washington: NASA), 73
Martin, S. F., Livi, S. H. B., & Wang, J. 1985, Australian J. Phys., 38, 885
Moore, R., Porter, J., Roumeliotis, G., Tsuneta, S., Shimizu, T., Sturrock, P. A., & Acton, L. W. 1994, in Proc. Kofu Symposium: A New Look at the Sun with Emphasis on Advanced Observations of Coronal Dynamics and Flares, ed. S. Enome & T. Hirayama (Nagano: Nobeyama Radio Obs.), 89
Moore, R. L., & Roumeliotis, G. 1992, in Eruptive Solar Flares, ed. Z. Svestka, B. V. Jackson, & M. E. Machado (Berlin: Springer), 69
Narain, U., & Ulmschneider, P. 1996, Space Sci. Rev., 75, 453
Parker, E. N. 1988, in Solar and Stellar Coronal Structure and Dynamics, ed. R. C. Altrock (Sunspot: Natl. Solar Obs.), 1
Porter, J., Moore, R., Roumeliotis, G., Shimizu, T., Tsuneta, S., Sturrock, P. A., & Acton, L. W. 1994, in Proc. Kofu Symposium: A New Look at the Sun with Emphasis on Advanced Observations of Coronal Dynamics and Flares, ed. S. Enome & T. Hirayama (Nagano: Nobeyama Radio Obs.), 65
Rabin, D., Moore, R., & Hagyard, M. J. 1984, ApJ, 287, 404
Rosner, R., Tucker, W. H., & Vaiana, G. S. 1978, ApJ, 220, 643
Roy, J.-R., & Michalitsanos, A. G. 1974, Sol. Phys., 35, 47
Shimizu, T., Tsuneta, S., Acton, L., Lemen, J., & Uchida, Y. 1992, PASJ, 44, L147
Solar-Geophysical Data. 1992 (Boulder: Nat'l Geophysical Data Center), vols. 570, 572, 577, 578, and 580
Teuber, D., Tandberg-Hanssen, E., & Hagyard, M. J. 1977, Sol. Phys., 53, 97
Tsuneta, S., et al. 1991, Sol. Phys., 136, 37
Vaiana, G. S., & Rosner, R. 1978, ARA&A, 16, 393
Webb, D. F., & Zirin, H. 1981, Sol. Phys., 69, 99
West, E. A. 1989, in Polarization Considerations for Optical Systems I (Bellingham: SPIE), 434
Zwaan, C. 1987, AR&A, 25, 83